De-risking Fluid Type in Unpenetrated Fault Compartment using Seismic Calibration, Erha Field, Offshore Nigeria

Sikiru A. Amidu, Patricia I. Ochogbu, Guy F. Medema, Felix O. Obere, and Christopher W. Drexler
Esso Exploration and Production Limited, Lagos, Nigeria

ABSTRACT

Oil field development in deep water settings is challenging and expensive. De-risking fluid type through seismic calibration can help support business decisions to evaluate and proceed with field and reservoir developments. Seismic calibration was employed to de-risk fluid type in an unpenetrated fault compartment in Erha field, using well data from adjacent fault block. Erha-1X well (drilled in a low side fault compartment) penetrated a deep water channel system east of the Erha Main field and encountered multiple pay intervals. The Me1 interval (oil in Erha 1X) was mapped to the southwest (SW) into a high-side unpenetrated fault compartment. In the absence of a well penetration, fluid type could not be de-risked completely. However, comparison of the seismic attributes between the two fault blocks gave supporting evidence of possible fluid type in the SW fault block. The seismic calibration process involved wedge modeling, amplitude variation with offset (AVO) modeling and seismic attribute analyses on stacked volume, seismic gathers and amplitude extractions. Wedge modeling showed that reservoir thickness was above maximum tuning, thus the observed amplitude was relatively characteristic of the reservoir. AVO modeling showed amplitude increase with offset for oil- and gas-filled reservoir cases. AVO analyses on stacked seismic sections, gathers, and extractions, showed Class III AVO for Me1 oil sand at Erha 1X, whereas in the Me1 SW fault block, different bright spots showed Classes III/IV AVO. AVO Class III with amplitude strength consistent with Me1 oil sand in Erha 1X was found at the upper side of Me1 SW close to major fault. The calibration results have been used as part of decision to propose a drill well location in the SW fault block.

Keywords: Seismic Calibration, Amplitude Variation with Offset (AVO), Deepwater, Niger Delta.

INTRODUCTION

The use of seismic calibration and AVO for direct hydrocarbon identification in deep water channel systems can help to quantify the risk during hydrocarbon prospecting (Rutherford and William, 1989; Roden *et al.,* 2014). Several case studies have shown successful use of AVO to drill productive wells (Hall, *et al.,* 1995; Roden *et al.,* 2012), whereas other failed cases have shown that clean porous, wet sands can cause AVO anomalies similar to those caused by gas sands in less porous blocks (Estill and Wrolstad, 1993; Loizou *et al.,* 2008). The aim of AVO analysis is to deduce rock properties of the subsurface from seismic data by differentiating lithology-related from hydrocarbon-related seismic anomalies. The underlying concept is that Poisson's ratio, or the related ratio of P-wave velocity to S-wave velocity (VP/VS), is significantly affected by pore fluid as the VP/VS of hydrocarbon-bearing sediments normally deviates from the VP/VS trend of the background rocks (Simmons and Backus, 1994; Dong, 1999). Ostrander (1984) combined these observations to show how the AVO reflection response can be used to distinguish seismic amplitudes caused by gas sands from bright reflection amplitudes caused by non-hydrocarbon-bearing rocks. Over the past decades, AVO has evolved from a relatively new technology to increasingly mature applications. Careful seismic data processing, detailed petrophysical modeling, and calibration to measured properties of target reservoir sands have demonstrated effectiveness (Hall *et al.,* 1995). Mature basins with the advantages of known analogs and where conventional amplitude anomalies have been tested; represent ideal conditions for regional and reservoir scale applications (Hall *et al.,* 1995).

The objective of this study was to de-risk fluid type in an un-penetrated fault compartment based on seismic response and well data from an adjacent fault block. This study was part of an integrative project aimed at generating drill well opportunities in the unpenetrated fault block. The study area is in the Erha field, which is in 1000 – 1200 m water depth, 60 miles offshore Niger Delta (Figure 1a). The Erha field consists of two major reservoirs - Erha Main and Erha North. Both are deep water Miocene slope channel complex systems with multiple channel sets. The Erha 1X well (drilled in the adjacent fault compartment) penetrated a deep water channel system east of the Erha Main field. The wells

The authors wish to thank Nigerian National Petroleum Corporation (NNPC) and Mobil Producing Nigeria Unlimited, Nigeria, for release of the materials and permission to publish this work. Many thanks to the Geoscience community of the Mobil Producing Nigeria Unlimited for technical reviews and suggestions.
NAPE Bulletin, V.29 No 1 (April 2020) P. 1-7

stacked multiple pay intervals with gas, oil and gas on oil. Brine filled sands were also found in some intervals (Figure 1b). The Me1 interval was penetrated and confirmed Class III AVO in Erha1X, and the same interval was mapped to the SW into a high-side fault compartment (Figure 1c). In the absence of any well penetration, seismic calibration, through AVO analysis, was identified as a method to predict fluid type in the SW fault block.

The study involved wedge and synthetic modeling as well as visual amplitude analysis on pre-stack and post-stack seismic data. The wedge and AVO modeling were proposed to validate the calibrated AVO response and estimate tuning thickness at Erha 1X. The required compressional (VP) and shear (VS) wave velocities for the modeling were based on in-situ data as both compressional and shear sonic logs were measured in Erha 1X. The AVO analysis on seismic data was proposed to highlight the similarities or differences from the SW fault block to the known rock and fluid response at Erha 1X. The AVO classification is based on Rutherford and William (1989). The study gave a supportive evidence of possible fluid type in the SW fault block. The result has been used, in collaboration with results from other studies, to propose a potential drill well location in the unpenetrated fault block.

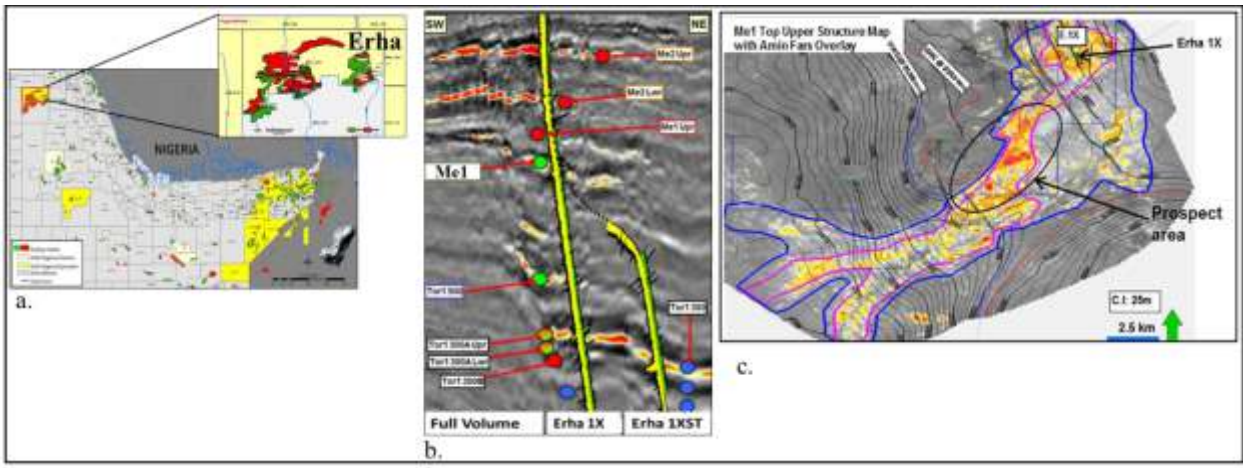

Figure 1: (a) Location map of Erha Field Offshore Nigeria; (b) Erha 1X well with penetrated sand intervals; and (c) Me1 top structure map with minimum amplitude extraction showing Me1 channel sand at Erha 1X and in the SW fault compartment.

METHODOLOGY

Wedge Modeling

A wedge model was created to forward model any possible effect of wavelet interference in resolving the Me1 sand layer on the seismic and to determine the tuning thickness, and by implication, evaluate the integrity of the bright spots on the Me1 sand. Based on our experience working in deep water setting, it is always advisable to build wedge model to evaluate possible thin layer effects as presence of a thin layer results in a change in both amplitude and the waveform of the reflected waves (Wides 1973, and Kallweit and Wood, 1982). The exact thickness for which maximum tuning occurs at normal incidence depends upon the shape of the incident waveform and the velocity of the layer itself (Juhlin and Young, 1993). Figure 2 shows the wedge model which was generated using the 2D Session module in RokDoc. VP-VS-Rho properties for the modelled overburden and underburden shale (colored blue), and Me1 sand wedge (colored yellow) were extracted from the Erha 1X log data. These input parameters are summarized in Table 1. The model is of a sand wedge encased within shale layers of higher compressional velocities (VP) and higher densities (Rho). Consistent with seismic processing report, the wedge was illuminated using a quadrature wavelet with dominant frequency of 25 Hz. The values were made constant for each layer so that only tuning effects would be observed (Dong, 1999). The location of Erha 1X in the model space, and thickness estimate as well as amplitude tuning curves that were measured from the modelled seismic response are also shown.

As shown in Figure 2, when the modelled sand layer is thick enough compared to the seismic wavelength, reflections from the top and bottom of the layer are independent of one another. Hence, the top and base of the model reservoir are imaged uniquely. However, as the sand thins, the reflection from the top of the sand wedge and the reflection from the base of the wedge interfere constructively with one another, making it increasingly difficult to distinguish the separate reflectors. For this model, the point of maximum constructive interference being the "maximum tuning point" was found to be around 16 m. The wedge model showed that the reservoir thickness (approximately 24 m) was greater than the

maximum tuning thickness, though the onset of tuning was found to be around 30 m. The observed amplitude of Me1 sand was by implication characteristic of the reservoir, though, it also showed that care should be taken when interpreting various bright spots on the seismic and attribute data.

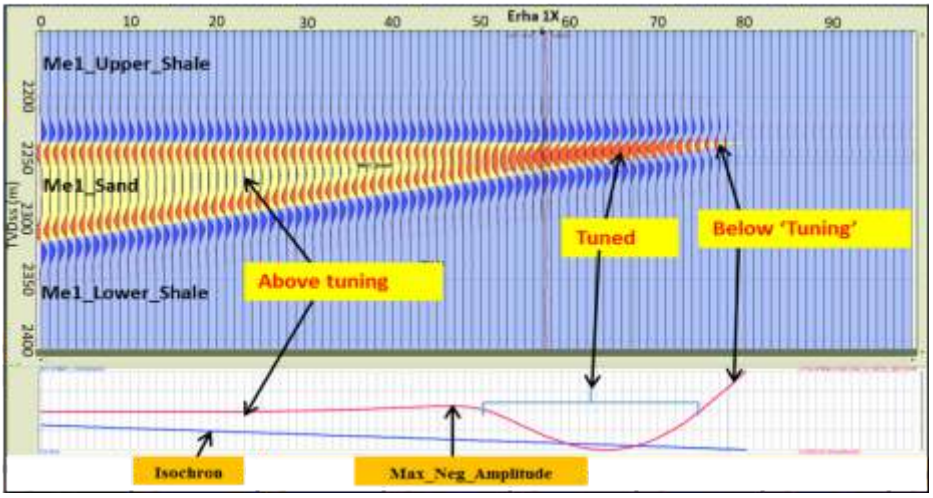

Figure 2: The wedge model to model thin layer effects using log data from Erha 1X.

Table 1: Elastic properties from Erha 1X log data that were used for the wedge modeling.

Layers/Properties	Vp (m/s)	Vs (m/s)	Rho (g/cm3)	Poisson's ratio
Me1 Oil Sand	2235	1028	2.06	0.366
Overlying shale	2300	948	2.24	0.393
Underlying shale	2450	1040	2.26	0.395

AVO Modeling

AVO modeling was carried out to further validate the AVO response of the Me1 oil sand at Erha 1X. The single interface AVO module in RokDoc was used. For comparative analysis, gas- and brine-filled reservoir cases were also employed using the shallower gas sand and deeper wet sand in Erha 1X. The modeling algorithm used the Zoeppritz equations, which relate the amplitude of P-wave, incident upon a plane interface, and the amplitude of reflected and refracted P- and S-waves to the angle of incidence (Simmons and Backus, 1994). The Erha 1X well logs were blocked at various depth-intervals to create shale-sand interfaces (Fig. 3a), then elastic properties were extracted and these were used as input into the modeling process. Figure 3b shows the modelled AVO response for the various shale-sand interfaces. For the Me1 oil sand (green), model shows low impedance amplitude response that brightens with offset, consistent with Class III AVO. Amplitude responses for the shallow gas sands (red and purple) are higher, but, also consistent with AVO Class III, as the amplitude brightens with offset. Brine case yields no response at near and very weak negative response at far angles (possible Class II AVO).

Amplitude Analysis on Seismic Data

Amplitude analysis based on seismic responses between the two fault blocks was carried out using stacked volumes and seismic gathers. The seismic data has been especially processed to preserve relative amplitude, phase and frequency spectrum (Finn and Winbow, 2002). Amplitude strengths and values on stacked volume and seismic gathers were calibrated at Erha 1X and results propagated unto the SW compartment. Figure 4a shows an arbitrary seismic section connecting the two fault blocks, around the Me1 sand and shallower Me2 gas sands. The seismic amplitude was scaled so that direct comparison of the amplitude strengths between the two sections could be carried out. The Me1 sand in the prospect area (yellow circle) shows relatively bright amplitude on the near volume and there is increase in amplitude to the far volume. The amplitude strength is consistent with penetrated and confirmed Me1 oil sand (blue circle) on the downthrown fault block. The observed AVO is consistent with AVO Class III

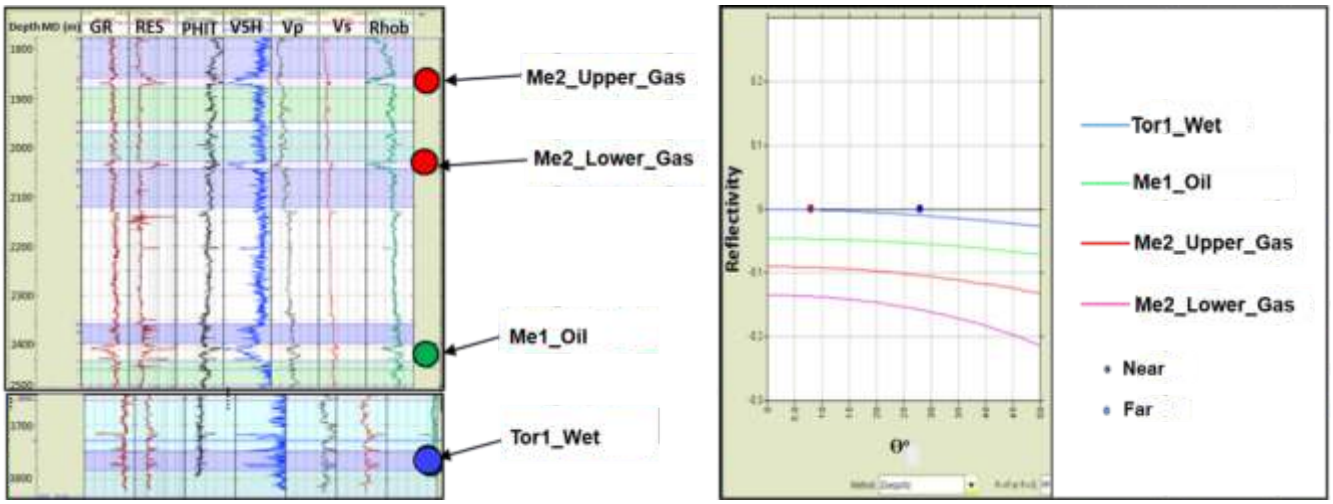

Figure 3: Synthetic AVO modeling using Erha 1X logs, (a) Erha 1X log data with , (b) modeled AVO response between top of sands and overlying shale for Me1 and representative sand layers penetrated by Erha 1X.

(Rutherford and William, 1989). The high amplitudes of the shallow gas sands that remain relatively flat with offset are also noticeable. This is consistent with AVO Class IV.

The minimum amplitude extractions on the near, mid and far angle stacks are shown in Figure 4b. Generally, the attribute extraction shows increase in amplitude with offset at Erha 1X and in the SW compartment; consistent with observation from stacked seismic section. Close to major fault, amplitude strength at Me1 SW (golden circle) is consistent with that for Me1 main compartment at Erha 1X (yellow circle). Meanwhile, far away from fault, isolated spots that remain relatively flat with offset (AVO Class IV) are observable in the Me1 SW compartment.

To further evaluate the observed AVO on the stacked volume, CMP (Common Mid-Point) gathers (in offset domain) were extracted at Erha 1X and in the SW block targeting identified bright spots on the amplitude extractions. The gathers were processed using Hampson-Russel (H-R) AVO modeling workflow to generate bandwidth-balanced angle gathers. Conversion from offset to angle gathers draws from the fact that seismic reflectivity at an interface is a function of reflection angle rather than offset, and amplitude analysis on angle gathers

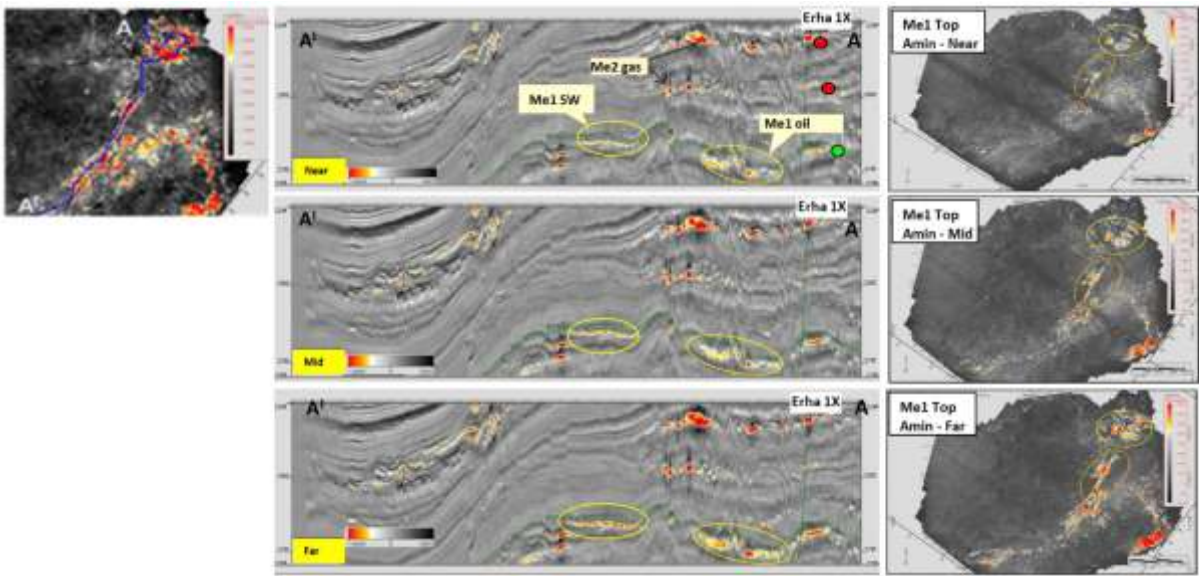

Figure 4: Variation in amplitude with offset on near, mid and far volumes: (a) stacked seismic volume and (b) minimum amplitude (Amin) attribute extractions.

(sometimes referred to as amplitude variation with angle – AVA) offers potential to better attenuate noise and to reveal relative amplitude variations contained in reflected signal (Resnick, 1993). The offset angles in this analysis range from 0 to 450. The workflow processing steps are shown in Figure 5. Time-velocity table was created using the time-depth relationship for Erha 1X and amplitude spectra were extracted over 1 second time window (0.5 second above and below the Me1 sand). The band pass filter was designed using frequency values from the amplitude spectra. Details of the processing steps are as explained by Resnick (1993).

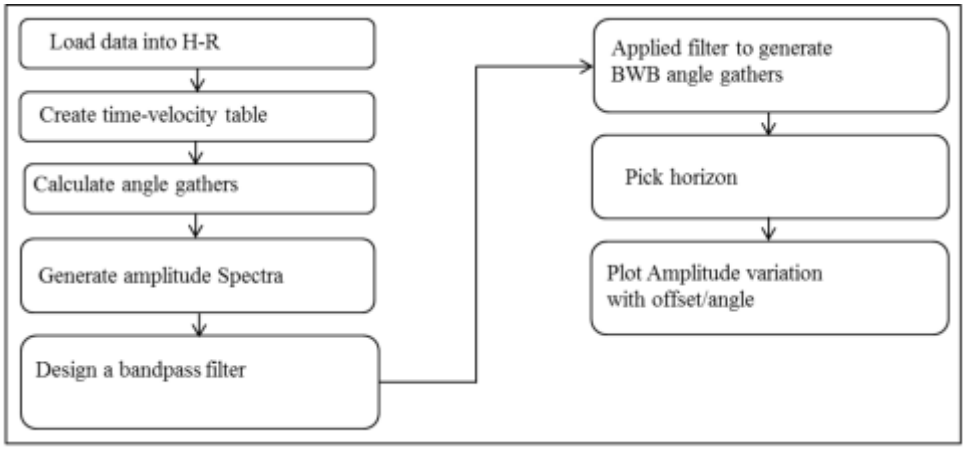

Figure 5: Workflow that was used for calculating angle gathers from raw time offset-varying CMP gathers to angle gathers in Hampson-Russel.

Figure 6 shows amplitude variation from near to far angles on the angle gathers in the Erha 1X and at identified bright spots in the SW fault block. At Erha 1X, the penetrated Me1 oil sand shows amplitude increase with offset; consistent with the AVO Class III that was observed on stacked volumes. In the SW fault block, seismic gathers from different bright spots show variable AVO responses for the Me1 sand. At designated Location L1, the Me1 sand shows AVO Class III and the amplitude strength is comparable with confirmed oil sand in Erha 1X. At Location L2, the Me1 sand shows AVO Class III/IV, whereas the Me1 sand at Location L3 shows a Class IV (flat with angle) response with very bright amplitudes on the nears out to the fars.

The observed AVO is quantitatively illustrated in Figure 7 (plots were also obtained from H-R AVO). At Erha 1X, amplitude (absolute) values start at around 6000 at near angles and increased to around 20000 at far angles for Me1 oil sand. The comparable amplitude values are found at L1 where amplitude ranges from about 10000 at near to about 25000 at far angles, consistent with qualitative AVO analysis in Figure 6. The amplitude values at Locations L2 and L3 start high (greater than 25000) and remain

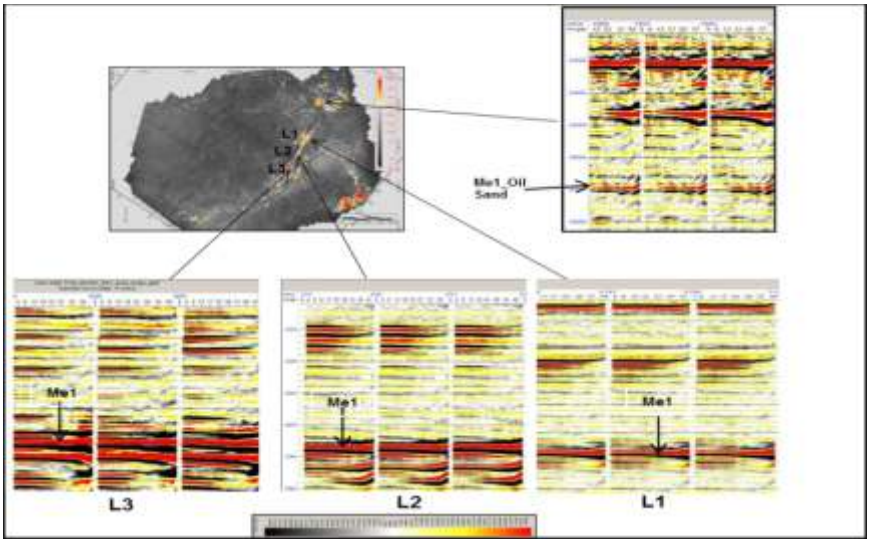

Figure 6: Comparison of AVO at Erha 1X oil sand and at representative bright spots in the SW fault block.

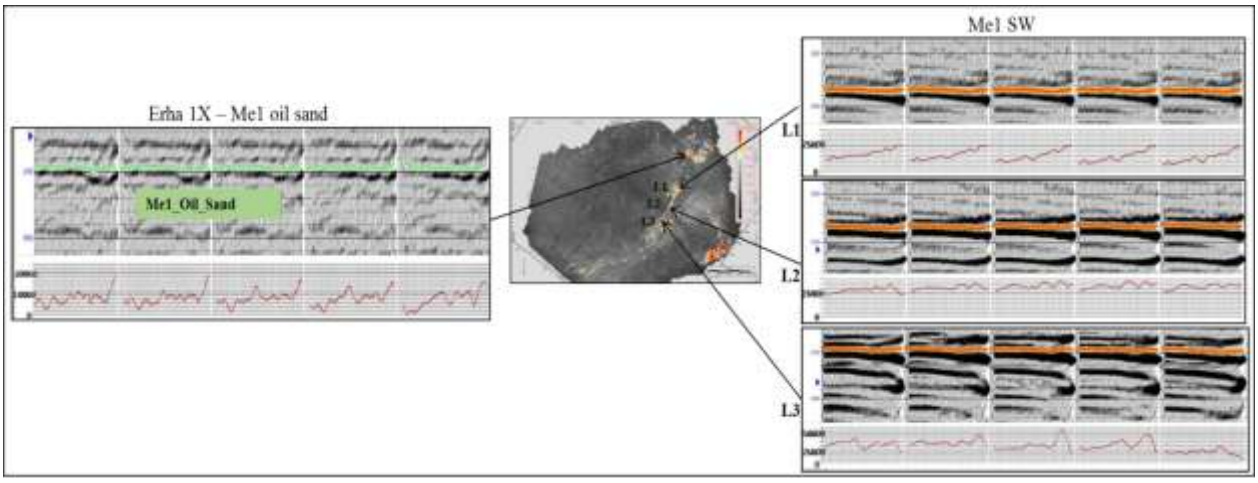

Figure 7: Quantitative plots of AVO shown in Figure 6

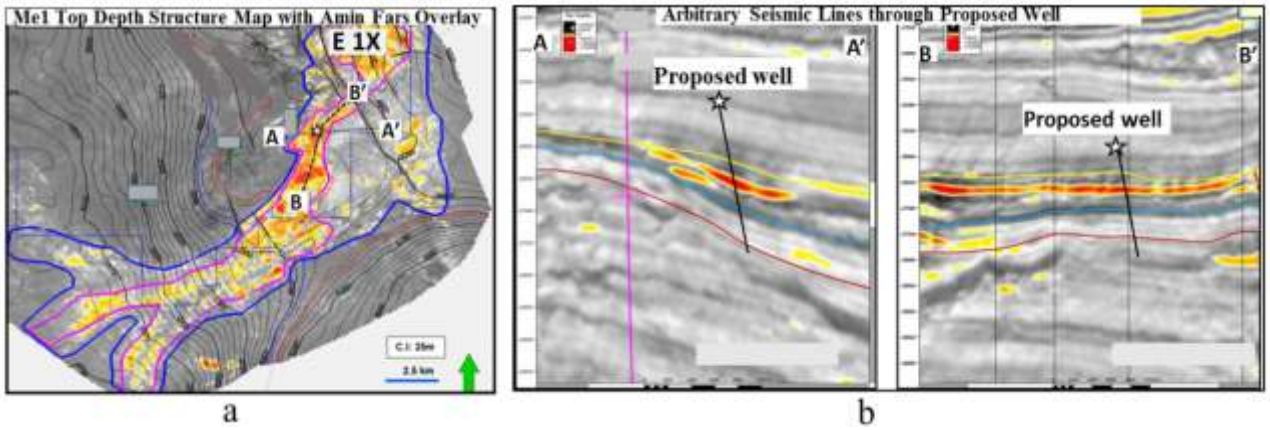

Figure 8: (a) Proposed drill well location; (b) Arbitrary seismic lines through the proposed well.

relatively constant from near to far angles.

DISCUSSION

Seismic calibration of an Me1 anomaly was carried out using seismic data and log. Wedge modeling shows reservoir thickness was above maximum tuning, though the sand thickness lied within the tuned wedge in the model. Synthetic AVO modeling in this study shows an expected AVO increase for oil and gas filled reservoir cases. AVO analyses on stacked seismic sections and attribute extractions show Class III AVO for Me1 oil sand at Erha 1X, and AVO Class III/IV in the Me1 SW. Corroborative evidence was provided by qualitative and quantitative amplitude analysis on seismic gathers from different bright spots. AVO Class III with amplitude strength relatively consistent with Me1 oil sand in Erha 1X was found at the upper side of Me1 SW close to major fault.

It is important to emphasize that, while the amplitude strength/AVO is consistent with the Me1 oil sand response at Erha 1X, Class III AVO is not necessarily 100% diagnostic for oil versus gas (Ostrander 1984; Rutherford and William, 1989). The results, however, are consistent with geological and other interpretations, which were part of this integrative project. For example, fluid contact mapping which was carried out independently has placed the comparable AVO sand in the SW within the oil leg in the fault compartment. Consequently, this calibration has been used in collaboration with results from other studies to propose a well location in the AVO Class III sand in Me1 SW. The proposed well and arbitrary seismic lines through the well location are shown in Figure 8.

CONCLUSION

The present study shows that AVO is an effective tool for opportunity generation in a deep water setting. The result also shows that, for accurate and reliable AVO results, careful data processing, and calibration to existing well data are necessary pre-requisites. Since AVO analysis is not foolproof (Ostrander 1984; Resnick, 1993), better integration of geological and geophysical interpretation is important. This is especially the case in this project, where despite the Me1 sand being inferred to be relatively tuned (as shown by wedge modeling); availability of geological information improved confidence on AVO results. Although this project has focused on a particular deep water sand in Erha field offshore Niger Delta, the approach to AVO analysis, as presented in this paper, should be applicable in many fields in other parts of the world, especially in mature fields where conventional amplitude anomalies have been tested and where well data are available for calibration. Consequently, many long-productive fields may benefit from a careful second look, where AVO tool could be used to derisk structural and stratigraphic traps that could have gone previously unnoticed.

REFERENCES CITED

Dong, W. (1999). AVO detectability against tuning and stretching artifacts, Geophysics, Vol. 64, No. 2, 494-503.

Estill, R. and Wrolstad, K. (1993). Interpretive aspects of AVO – application to offshore Gulf Coast bright spot analysis, In: Castagna, J. P. and Backus, M. M. (eds). Offset-Dependent Reflectivity - Theory and Practice of AVO Analysis, Society of Exploration Geophysicists, p. 267 -284.

Finn, C. J. and Winbow, G. A. (2002). Method for controlled-amplitude prestack time migration of seismic data; US Patent Number: US 6446007 B1.

Hall, D. J., Adamick, J. A., Skoyles, D., DeWildt, J. and Erickason J. (1995). AVO as an exploration tool: Gulf of Mexico case studies and examples. The Leading Edge, Vol. 14, No. 8, p 863 –869.

Juhlin, C., and Young, R. (1993). Implications of thin layers for amplitude variation with offset (AVO) studies. Geophysics, Vol. 58, No. 8, p 1200-1204.

Kallweit, R. S. and Wood, L. C. (1982). The limits of resolution of zero-phase wavelets. Geophysics, Vol. 47, No. 7, p 1035 - 1046.

Loizou, N., Liu, E. and Chapman, M (2008). AVO analyses and spectral decomposition of seismic data from four wells west of Shetland, UK. Petroleum Geoscience, Vol. 14, p 355-368.

Ostrander, W. J. (1984). Plane-wave reflection coefficients for gas sands at non-normal angles of incidence. Geophysics, Vol. 49, No. 10, p 1637-1648.

Resnick, J. R. (1993). Seismic data processing for AVO and AVA analysis, In: Castagna, J. P., and Backus, M. M. (eds). Offset-Dependent Reflectivity-Theory and Practice of AVO Analysis. Society of Exploration Geophysicists, p. 175 - 189.

Roden, R., Forrest, M. and Holeywell, R. (2012). Relating seismic interpretation to reserve/resource calculations: Insights from a DHI consortium. The Leading Edge, Vol. 31, p 1066–1074.

Roden, R., Forrest, M., Holeywell, R., Carr, M. and Alexander, P. A. (2014). The role of AVO in prospect risk assessment, Interpretation, Vol. 2, No. 2, p SC61-SC76.

Rutherford, S. R. and Williams, R. H. (1989). Amplitude-versus-offset variations in gas sands, Geophysics, Vol. 54, No, 6, p 680--688.

Simmons Jr., J. L., and Backus, M. M. (1994). AVO modeling and the locally converted shear wave, Geophysics, Vol. 59, No. 9, p 1237-1248.

Wides, M. B. (1973). How thin is a thin bed? Geophysics, Vol. 38, No. 6, p 1176-1180.


NIGERIAN ASSOCIATION OF
SINCE
1975
PETROLEUM EXPLORATIONISTS